Radiation Physics and Chemistry 167 (2020) 108224

Contents lists available at ScienceDirect

Radiation Physics and Chemistry

journal homepage: www.elsevier.com/locate/radphyschem

A theoretical model for the cross section of the proton-boron fusion nuclear reaction

Federico Alejandro Geser[a,b,*], Mauro Valente[a,b,c]

[a] Instituto de Física Enrique Gaviola, CONICET, Córdoba 5000, Argentina
[b] Laboratorio de Investigaciones e Instrumentación en Física Aplicada a la Medicina e Imágenes por Rayos X - LIIFAMIR, FAMAF, Universidad Nacional de Córdoba, Córdoba 5000, Argentina
[c] Centro de Física e Ingeniería en Medicina CFIM, Departamento de Ciencias Físicas, Universidad de la Frontera, Temuco 4780000, Chile

ARTICLE INFO

Keywords:
Reaction cross section
Proton-boron fusion
Proton therapy

ABSTRACT

This work proposes a theoretical estimation for the cross section of the proton-boron fusion reaction for the first excited level of the beryllium intermediate nucleus, based on nuclear theories for isolated resonances and continuum reaction cross sections that acceptable reproduce available experimental data. This result might help to analytically deconvolute the alpha particles contribution from the total dose in the mixed field of the irradiation in biological tissue, and might also be useful for applications in aneutronic energy sources research.

1. Introduction

Therapy with charged particle ions, and particularly with protons, is a modality for treatment of cancer diseases aimed at irradiation of in-depth localized tumors. Moreover, it has also proven to be feasible for infant patients (Vogel et al., 2017). Localized energy deposition is desirable for dose conformation in these cases, and the inverse depth-dose profile (the Bragg curve) is quite ideal. More recently (Yoon et al., 2015; Shin et al., 2016), an improvement of the technique was proposed, consisting of using the boron 11 (^{11}B) isotope to induce a nuclear reaction called proton-boron fusion (capture). The proton-boron fusion reaction was first studied by Oliphant and Rutherford in 1933 (Oliphant and Rutherford, 1933). Since then, several researchers proposed models for the cross section for different configurations of the reaction process. The interest in this reaction is mainly based on the possibility of using it as an aneutronic energy source, but in the last years, a potential improvement of cancer therapies using protons was proposed, mainly based on the positive Q-value of the reaction. The final state of this reaction consists of three alpha particles with energies around 4 MeV having high linear energy transfer (LET), and there is a non-negligible probability of emission of a mono-energetic prompt gamma photon (Petringa, 2017). Therefore, dose enhancement together with on-line monitoring of the irradiation process seem feasible. Moreover, the first dose modifying factors have been measured experimentally for non-toxic concentrations of boron in vitro (Cirrone et al., 2018), although the reasons of the reported improvement are not very well understood yet.

Becker et al. (1987) proposed that the proton-boron fusion (PBF) nuclear reaction predominantly proceeds via sequential decay with an intermediate 8-beryllium (^{8}Be) nucleus, usually denoted as $^{11}B(p,\alpha)^{8}Be^{*}$. More recently in 2009, it has been stated by Dmitriev (2009) that the mean life time of the first excited state of this ^{8}Be is extremely short, and therefore it decays before leaving the strong interaction range, supporting the direct break-up of the compound carbon 12 (^{12}C) nucleus in three alpha particles. Nevertheless, modeling the reaction using the beryllium is plausible and useful to estimate the cross section (as a measurement of the occurrence probability) for the PBF.

In this work, the reaction cross section for PBF is determined using the nuclear reaction theories for continuum and resonance peaks, depending on the energy range. These theories are standard in nuclear physics (Blatt and Weisskopf, 1979; Wong, 2007; Bertulani, 2013), and require knowledge of the particle's dynamics (Wang et al., 2017), the different decay widths associated to the resonance peaks (Ajzenberg-Selove, 1990; Kelley et al., 2017), and the mathematical properties of the solution of the Schrdinger's equation with Coulombian interaction term (Abramowitz and Stegun, 1964).

2. Theory and model

The type of reaction intended to be described is of the form

* Corresponding author.
E-mail address: fgeser@famaf.edu.ar (F.A. Geser).

https://doi.org/10.1016/j.radphyschem.2019.03.028
Received 26 November 2018; Received in revised form 19 March 2019; Accepted 21 March 2019
Available online 25 March 2019
0969-806X/

$a + \mathbb{X} \longrightarrow b + \mathbb{Y}$, where a is the projectile (usually a nucleus or nucleon) that generates a reaction with target nucleus $\mathbb{X}$. b is usually called the product of the reaction, and $\mathbb{Y}$ the residual nucleus, in this case, beryllium is known as the entrance channel of the reaction $\alpha = a + \mathbb{X}$, with energy ε_α. PBF has a Q-value given by:

$$Q = (m_a + m_{\mathbb{X}} - (m_b + m_{\mathbb{Y}}))c^2 = 8.59\, MeV \tag{1}$$

being an exothermic reaction. The probability that the entrance channel "chooses" one of the available exit ones is known as the *reaction cross section* for that specific process. If the results of the reaction are the constituents of the entrance channel, an elastic reaction has occurred. Therefore, the cross section must have this possibility into account, that is $\sigma = \sigma_{elas} + \sigma_r$, where σ_r is the inelastic reaction cross section. If α is the entrance channel, then:

$$\sigma_r = \sum_{\beta \neq \alpha} \sigma(\alpha, \beta) + \sigma_{cap}(\alpha) \tag{2}$$

where σ_{cap} is the probability that the projectile initiates a capture reaction without emission of further particles in the exit channel other than a compound nucleus. $\sigma(\alpha, \beta)$ is defined as:

$$\sigma(\alpha, \beta) = \frac{\text{number of emissions in channel } \beta \text{ per unit of time and per nucleus } \mathbb{X}}{\text{number of incident particles in channel } \alpha \text{ per time and area units}}. \tag{3}$$

This is the cross section of interest for this work, that is modelled according to the energetic region analyzed, whether it is the continuum region or a resonance peak. In both cases, a definite nuclear surface is assumed to exist.

The elastic scattering is easily solvable by means of quantum mechanics calculations. Making the spherical harmonics decomposition of the plane wave with the ${Y_l}^0(\Omega)$ functions, the cross section could be evaluated by means of the phase change $\delta_l(\vec{k})$ in the spherical outgoing wave:

$$\sigma_{elas}(\alpha) = \sum_{l=0}^{\infty} \sigma_{elas,l} \quad ; \quad \sigma_{elas,l} = \frac{\pi}{k^2}(2\,l + 1)|1 - \eta_l|^2 \quad ; \quad \eta_l = e^{i\delta_l\left(\vec{k}\right)}. \tag{4}$$

This is the result of the partial wave decomposition treatment of scattering as presented in any quantum mechanics textbook (Merzbacher, 1998; Cohen-Tannoudji et al., 2006; Garcia and Galindo, 1991).

Committing to the reaction cross section, it might be thought of as the number of initial particles a that can get into a sphere of radius R where the nuclear potential is effective ($|\vec{r_a} - \vec{r_{\mathbb{X}}}| < R$), but not leave it. The net flux of this wave can be calculated with the current probability:

$$N_a = -\frac{\hbar}{2im_\alpha} \int \left(\frac{\partial \psi}{\partial t}\psi^* - \frac{\partial \psi^*}{\partial r}\psi\right) R^2 \sin(\theta) d\theta d\phi, \tag{5}$$

where m_α is the reduced mass of the entrance channel.

The expression of the incident wave affected by the interaction potential, assumed to be central, can be written as:

$$\psi_{in}(r) \sim \frac{1}{2i} \sum_{l=0}^{\infty} (2\,l + 1) i^l\, P_l(\cos(\theta)) \frac{\eta_l e^{i\left(kr - \frac{l\pi}{2}\right)} - e^{-i\left(kr - \frac{l\pi}{2}\right)}}{kr}. \tag{6}$$

Here P_l are the Legendre polynomials. With all this, the reaction cross section can be calculated as:

$$\sigma_r(\alpha) = \frac{N_a}{N} = \frac{\pi}{k^2} \sum_{l=0}^{\infty} (2\,l + 1)(1 - |\eta_l|^2), \tag{7}$$

where N is total flux of the entrance channel, and its value corresponds to the relative velocity between a and $\mathbb{X}$.

If the Coulombian interaction between a and $\mathbb{X}$ is taken into account, the Schrdinger's equation has the form:

$$\nabla^2 \psi(\vec{r}) + \left\{k^2 - \frac{2m_\alpha}{\hbar^2} V(r)\right\} \psi(\vec{r}) = 0, \tag{8}$$

where $r = |\vec{r_a} - \vec{r_{\mathbb{X}}}|$ is the relative coordinate, m_α is the reduced mass of the entrance channel, $k = \frac{\sqrt{2m_\alpha \varepsilon_\alpha}}{\hbar}$ and $V(r) = \frac{1}{4\pi\varepsilon_0}\frac{Z_a Z_{\mathbb{X}} e^2}{r}$. The corresponding radial reduced equation for this with $\psi(\vec{r}) = R_l(r)P_l(\cos(\theta)) = \frac{u_l(r)}{r}P_l(\cos(\theta))$ is:

$$\frac{d^2 u_l}{dr^2}(r) + \left\{k^2 - \frac{l(l+1)}{r^2} - \frac{2m_\alpha}{\hbar^2} V(r)\right\} u_l(r) = 0 \quad (r > R). \tag{9}$$

Introducing $\rho = kr$ and the **Sommerfeld parameter** weighting the Coulomb interaction importance:

$$\gamma = \frac{Z_a Z_{\mathbb{X}} e^2}{4\pi\varepsilon_0 \hbar}\sqrt{\frac{m_\alpha}{2\varepsilon_\alpha}} = \frac{Z_a Z_{\mathbb{X}} e^2}{4\pi\varepsilon_0 \hbar v_\alpha}, \tag{10}$$

where v_α is the relative velocity in the entrance channel, radial reduced Eq. (9) might be written as:

$$\frac{d^2 u_l}{d\rho^2} + \left[1 - \frac{l(l+1)}{\rho^2} - \frac{2\gamma}{\rho}\right] u_l = 0. \tag{11}$$

This equation presents a pair of linearly independent solutions known as the **"regular" and "irregular" Coulomb wave functions** $F_l(r)$ and $G_l(r)$, depending on the confluent hypergeometric functions of the first kind ${}_1F_1(a\ ;\ b\ ;\ z)$:

$$F_l(\rho, \gamma) = C_l(\gamma)\rho^{l+1}e^{-i\rho}\ {}_1F_1(l + 1 - i\gamma\ ;\ 2\,l + 2\ ;\ 2i\rho), \tag{12}$$

$$G_l(\rho, \gamma) = \frac{2\gamma}{C_0^2(\gamma)} F_l(\rho, \gamma)\left\{\ln(2\rho) + \frac{q_l(\gamma)}{p_l(\gamma)}\right\} + \frac{1}{(2\,l + 1)C_l(\gamma)}\rho^{-l}\sum_{k=-l}^{\infty} a_k^l(\gamma)\rho^{k+l}, \tag{13}$$

where the functions $\{q_l(\gamma),\ p_l(\gamma),\ a_k^l(\gamma)\}$ can be seen in Abramowitz and Stegun table (Abramowitz and Stegun, 1964) and:

$$C_l(\gamma) = \frac{2^l e^{-\frac{\pi\gamma}{2}}|\Gamma(l + 1 + i\gamma)|}{\Gamma(2\,l + 2)}, \tag{14}$$

Making lineal combinations of these functions, the radial ingoing and outgoing spherical partial waves can be constructed:

$$u_l^+(r) = \exp(-i\sigma_l)[G_l(r) + iF_l(r)], \tag{15}$$

$$u_l^-(r) = \exp(i\sigma_l)[G_l(r) - iF_l(r)], \tag{16}$$

Thereby, in the outside the nucleus region $r > R$, the final solution of Eq. (9) can be written as:

$$u_l(r) = au_l^-(r) + bu_l^+(r). \tag{17}$$

Comparison with the asymptotic solution of Eq. (6) allows to determine a and b:

$$a = i^{l+1}(2\,l + 1)^{1/2}\frac{\sqrt{\pi}}{k} \quad ; \quad b = -\eta_l a. \tag{18}$$

Thereby, η_l must be determined by conditions inside the nucleus surface, but the same boundary condition will be applied in this case, also defining a condition for u_l^+ completely determined by conditions outside the nuclear surface:

$$f_l = R\frac{1}{u_l}\frac{du_l}{dr}\bigg|_{r=R}, \tag{19}$$

$$\Delta_l + is_l = R\frac{1}{u_l^+}\frac{du_l^+}{dr}\bigg|_{r=R}. \tag{20}$$

The f_l are known as excitation functions, and Δ_l and s_l depend entirely on the wave number k, the channel radius R, the angular momentum l and the Sommerfeld factor γ. With all this information it becomes possible to evaluate:

$$u_l^+(r) = \exp(-i\sigma_l)[G_l(R) + iF_l(R)], \tag{21}$$

$$\frac{du_l^+}{dr} = \exp(-i\sigma_l)\left[\frac{dG_l}{dr}(R) + i\frac{dF_l}{dr}(R)\right], \tag{22}$$

Then, the calculation gives: $\frac{1}{u_l^+}\frac{du_l^+}{dr}\Big|_{r=R} = \frac{1}{R}(\Delta_l + is_l)$, where:

$$\Delta_l = R\left[\frac{dG_l}{dr}(R)G_l(R) + \frac{dF_l}{dr}(R)F_l(R)\right]v_l, \tag{23}$$

$$s_l = R\left[\frac{dF_l}{dr}(R)G_l(R) - \frac{dG_l}{dr}(R)F_l(R)\right]v_l. \tag{24}$$

Here, the **penetration factor** $v_l = (G_l^2(R) + F_l^2(R))^{-1}$ was introduced. Introducing the phase of u_l^- with respect u_l^+ at $r = R$:

$$\exp(2i\xi_l) = \frac{u_l^-(R)}{u_l^+(R)} = \frac{G_l(R) - iF_l(R)}{G_l(R) + iF_l(R)}\exp(2i\sigma_l), \tag{25}$$

η_l can be obtained using values of Δ_l, s_l and ξ_l, as follows:

$$\eta_l = \frac{f_l - \Delta_l + is_l}{f_l - \Delta_l - is_l}\exp(2i\xi_l). \tag{26}$$

Therefore, the reaction cross section is:

$$\sigma_{r,l} = \frac{\pi}{k^2}(2\,l+1)\frac{-4s_l\mathbb{I}mf_l}{(\mathbb{R}ef_l - \Delta_l)^2 + (\mathbb{I}mf_l - s_l)^2}, \tag{27}$$

It is worth noting that as $\mathbb{I}mf_l < 0$, then $\sigma_{r,l} > 0$.

2.1. Continuum reaction cross section

For the continuum aproximation, it is necessary to assume that:

- If the projectile a penetrates the nuclear surface, it moves with kinetic energy $T_{in} \gg \epsilon_\alpha$. In fact, it can be considered that $T_{in} \approx \epsilon_\alpha + T_0$ where $T_0 \sim O(20\,MeV)$, according to typical intranuclear kinetic energy.
- This happens because inside the nucleus, the projectile is subject of the strong interaction, exchanging energy extremely fast with other nucleons.
- If a is a charged particle, it is convenient to assume the existence of several open exit channels.

The last condition is achieved if ϵ_α is much greater than the mean excitation energy of the target nucleus $\mathbb{X}$, with $Q > 3\,MeV$. This implies that there is a small probability that the exit channel is the same as the entrance one. Therefore, it is possible to assume that inside the nucleus, the solution to the reduced radial Schrdinger equation in the α channel behaves as $u_l \sim \exp(-iKr)$ when $r < R$. This means that the excitation functions satisfy $f_l = -iKR$ finally obtaining:

$$\sigma_{r,l}(\alpha) = \frac{\pi}{k_\alpha^2}(2\,l+1)\frac{4s_lKR}{\Delta_l^2 + (KR + s_l)^2}. \tag{28}$$

The s_l and Δ_l functions depends explicitly on the **Coulomb wave functions** that are solutions of the reduced radial Schrdinger equation with Coulombian potential (hypergeometric functions).

2.2. Resonance Breit-Wigner formula

In this case, the cross section is studied locally around those energy values where resonance exists. Unlike the continuous approximation, there exists an outgoing wave from inside the nuclear surface in the form $u_l \sim e^{-iKr} + be^{iKr}$ when $r < R$. This assumptions leads to the known formula of resonance in **Breit-Wigner** cross section for one level:

$$\sigma_{r,l}(\alpha) = \frac{\pi}{k_\alpha^2}(2\,l+1)\frac{\Gamma_\alpha^s\Gamma_\beta^s}{(\epsilon_\alpha - \epsilon_s^*)^2 + \left(\frac{1}{2}\Gamma^s\right)^2}, \tag{29}$$

where $\Gamma_{\alpha,\beta}$ and Γ^s are the partial and total decay widths respectively, and ϵ_s^* are the resonance energies.

3. Experimental data for PBF

For the PBF reaction, the simplest example of the clustering behavior of nuclei is the decay of the ground state of ^8Be into two α-particles. One explanation of this phenomenon is that nucleons prefer to form α-particle clusters in nuclei. Since the binding energy per nucleon of an α-particle is approaching the maximum value that can be attained inside a nucleus, there is relatively little force of attraction left between different α-particle "clusters". In the case of ^8Be, the binding energy actually favors the formation of two separate α-particles. For this reason, the ^8Be ground state is unstable toward α-particle emission ($\tau_{\frac{1}{2}} = 6.7 \times 10^{-17}\,s$), even though it is stable for β-decay and nucleon emission (Wong, 2007). Excited states of the ^8Be nucleus also show this tendency to decay via alpha emission. In fact, for all of the exit channels of the reaction $^{11}B(p,\alpha)^8Be$, the state is conformed by three alpha particles, and this fixes the amount of variables needed to the kinematical description of the observed alpha spectra. Nevertheless, the energy limits and other kinematical characteristics depend strongly on which of the exit channels is being observed. The possibilities are:

$$p + {}^{11}B \longrightarrow {}^{12}C^* \longrightarrow \alpha_0 + {}^8Be \longrightarrow \alpha_0 + \alpha_{01} + \alpha_{02} \tag{30}$$

$$p + {}^{11}B \longrightarrow {}^{12}C^* \longrightarrow \alpha_1 + {}^8Be^* \longrightarrow \alpha_1 + \alpha_{11} + \alpha_{12} \tag{31}$$

$$p + {}^{11}B \longrightarrow {}^{12}C^* \longrightarrow \alpha_2 + \alpha_3 + \alpha_4 \tag{32}$$

Except the last channel with three alpha particles appearing, the other two consist of a two step process in which the compound $^{12}C^*$ nuclei suffers an alpha decay with a residual nuclei corresponding to a ground or excited stated of a beryllium isotope. The reaction proceeds predominantly by sequential two-body decays via $^8Be^*(0,\ 3.03)$ (Kelley et al., 2017).

The proposed approach consists on assuming that the incident proton beam will be assumed to be unpolarized, and the corresponding average must be included in the cross sections. This also means that every incident proton can be in any of its spin $s = 1/2$ states, assuming also that the orbital angular momentum $\hat{L}$ corresponds to an S-wave with $l = 0$ or P-wave with $l = 1$ (only for the continuum aproximation). On the other hand, the ^{11}B in its ground state presents $\hat{I} = 3/2^-$. Therefore, the entrance **channel spin** is $\hat{S} = \hat{s} + \hat{I}$. In this reaction, this assumes the value $S = 2$. If $l = 0$ for incident protons, the total angular momentum of the compound nucleus $\hat{J} = \hat{S} + \hat{L}$ assume the values $J = S = |s - I|,\ ...,s + I = 1,\ 2$. Then, if the incident proton beam in the boron bulk is mainly composed of $l = 0$ protons, the only possible values for the angular momentum of the compound $^{12}C^*$ nucleus are

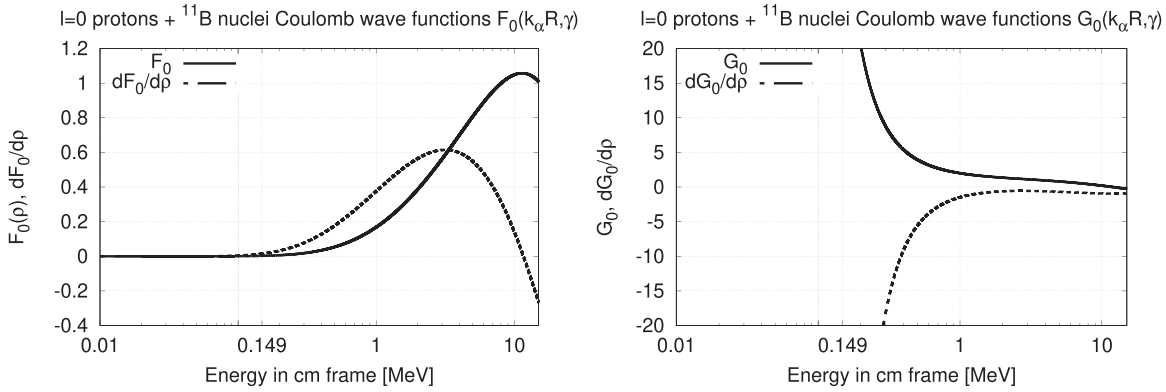

Fig. 1. Coulomb S-wave function and corresponding derivative up to 15 MeV, highlighting that $G_0(\rho, \gamma)$ is irregular at $\rho = 0$.

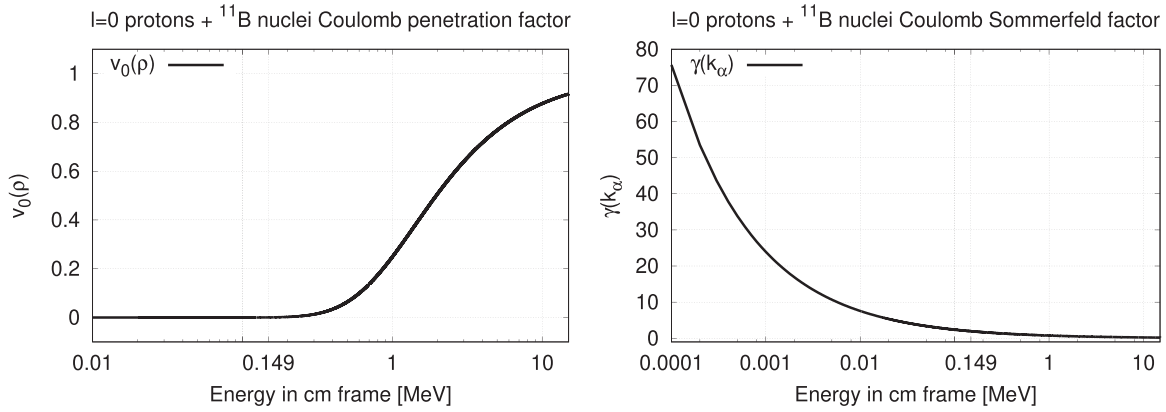

Fig. 2. Coulombian penetration factor for the $^{11}B(p, \alpha_1)^8Be$ reaction up to 15 MeV (left) and corresponding Sommerfeld factor (right).

$J = 1, 2$. Therefore, it is able to decay through any of the available channels and the this beryllium isotope can be obtained in its ground state or in the 3.03 MeV excited state only as a decay product of the excited $^{12}C^*$ compound nucleus with $J = 1, 2$.

Besides, the resonance peaks reached by this angular momentum restriction, and that will consequently be modelled with the theory, are summarized in the following table (Kelley et al., 2017), together with other possible resonant states that appear in the experimental data.

4. Results and discussion for the $^{11}B(p, \alpha_1)^8Be^*(3.03)$ reaction channel

In this section, results of Eq. (31) will be presented and discussed. Calculations were preformed using the *mpmath* library, a free (BSD licensed) *Python* library for real and complex floating-point arithmetic with arbitrary precision, capable on handling Coulomb wave functions and their derivatives.[1]

4.1. Results from continuum theory for S-wave state

The incident beam will be assumed to be composed mainly of $l = 0$ orbital angular momentum protons. The internal kinetic energy of the nucleons was approximated by the typical nuclear well with depth $-U_0$. This quantity can be modified by taking into account more realistic potential models, for example *optical model* that includes the spin-orbit interaction, the existence of a nuclear skin-depth (potential diffuseness in the surface, or Woods-Saxon potential) and the Coulomb interaction inside the nuclear surface. The different models approximate the behavior as a function of the distance r, meaning they are central potentials and thereby only changing the strenght of the potential well in the surface (Stock, 2009). The quantities that depend on the value of the potential in the continuum approximation only do so at the nuclear surface, i.e. the only value that changes if modifying the model inside the nucleus is the U_0 used to calculate K. Therefore, appropriate selection of U_0 value helps for approaching experimental data. The typical $U_0 = 42\ MeV$ is a good order of magnitude for the potential strenght at the nuclear surface, as will be seen.

Due to the focused interest on energies around 3 MeV, each of the quantities defined above were calculated up to 15 MeV, using the center-of-mass energy of the entrance channel with a step of $\Delta\varepsilon_\alpha = 100\ eV$. The Coulomb wave functions evaluation with the corresponding first order derivative are reported in Fig. 1.

These functions should lead to a penetration factor approaching to unity when increasing the energy, as can be confirmed in Fig. 2, along with the Sommerfeld factor γ, which is also shown as a function of the entrance channel energy.

Combining results for continuum S- and P- wave states, the results obtained through all the possible values of energy are reported in Fig. 4. As expected, only the high energy part (at least greater than 1 MeV) of the calculation can be thought of as a good aproximation.

[1] http://mpmath.org/.

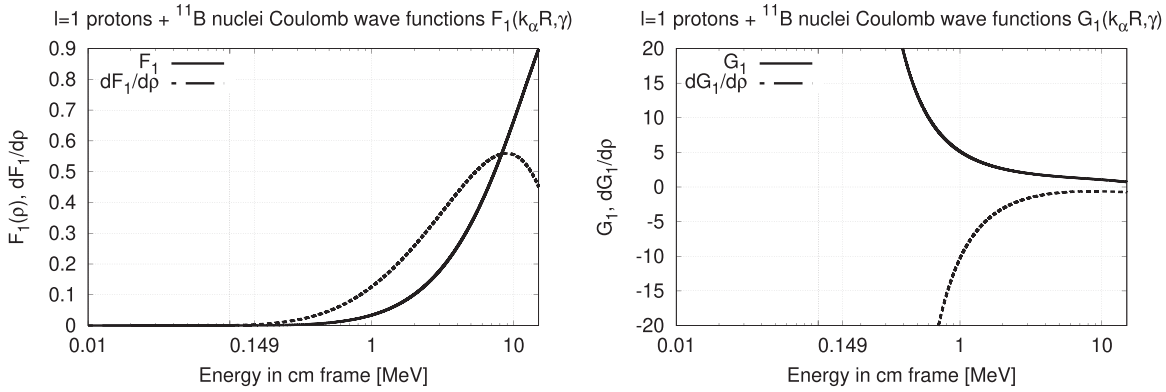

Fig. 3. Coulomb P-wave function and corresponding derivative up to 15 MeV, highlighting that $G_1(\rho, \gamma)$ is irregular at $\rho = 0$.

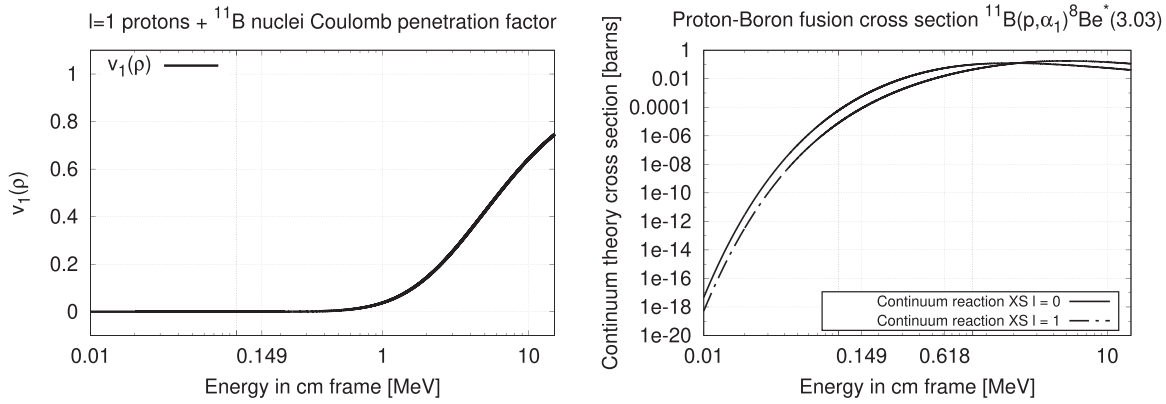

Fig. 4. Coulombian penetration factor for the $l = 1$ protons, with the corresponding theoretically calculated cross section for the $^{11}B(p, \alpha)^{8}Be^{*}(3.03)$ reaction channel via continuum theory for $l = 0$ and $l = 1$ protons.

Table 1
Resonance phenomenological parameters.

Proton Energy [keV]	Total width [keV]	Reaction width α_0 channel [keV]	Reaction width α_1 channel [keV]	Channel width [keV]	^{12}C level energy [MeV] and J^{π}
162	5.3 ± 0.2	0.26 ± 0.03	5.0 ± 0.2	0.0215 ± 0.0033	16.1060 ± 0.0008 ; 2^{+}
675	300	<0.27	150	150	16.576 ; 2^{-}
1388	1150	10	140	1000	17.320 ; 1^{-}
2640	≈ 400	65	177	68	18.38 ; 3^{-}
3750	1100	20	450	450	19.39 ; 2^{+}

It is important to keep in mind that the low energy part of this curves is at first not representative of the real cross section, because this estimation was obtained using the continuum theory of nuclear reactions. Nevertheless, the reaction cross section predicts a behavior comparable to the experimental measurements, and it may be used outside the resonance regions.

4.2. Results from continuum theory for P-wave states

If protons with $l = 1$ are assumed, maintaining all other parameters unchanged with respect to S-wave state, the corresponding Coulomb wave functions are reported in Fig. 3.

The Sommerfeld parameter remains the same as it does not depend on the angular momentum of the proton, but the penetration factor grows a little lower respect the $l = 0$ case. The cross sections are presented in Fig. 4, and again they might not be representative at low energy, but the reaction cross section can be added to the $l = 0$ case, enhancing the approximation to the experimental data.

4.3. Results from the resonances for α_1 emission

All resonances present for the $^{11}B(p, \alpha)^{8}Be^{*}(3.03)$ reaction channel were modelled with the Breit-Wigner one level formula (29).

The input data used were retrieved from different reports on light

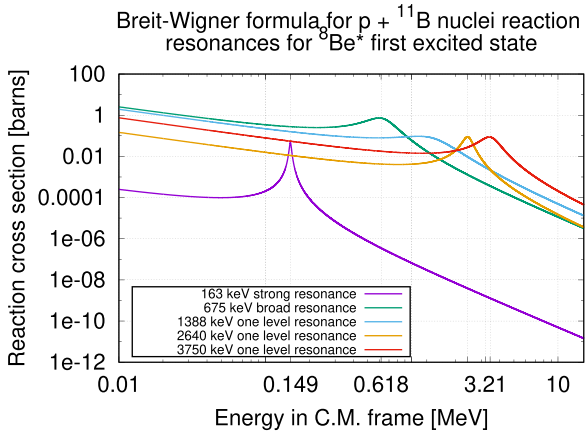

Fig. 5. Estimation of reaction cross section for the $^{11}B(p,\alpha)^{8}Be^{*}(3.03)$ reaction channel for isolated resonances.

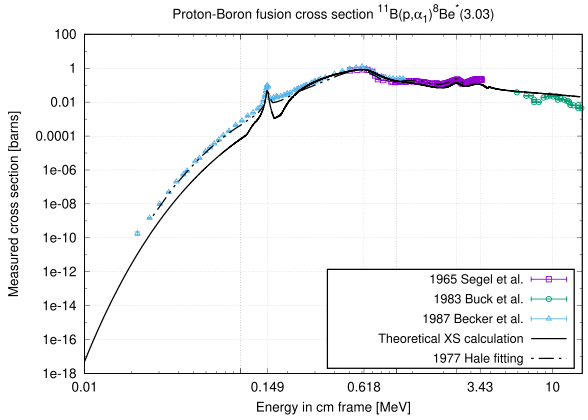

Fig. 6. cross section theoretical estimation for $^{11}B(p,\alpha)^{8}Be^{*}(3.03)$ reaction, compared with the Hale fitting of 1977 and the experimental data.

nuclei energy levels (Ajzenberg-Selove, 1990; Kelley et al., 2017) as summarized in Table 1, and only the α_1 channel widths corresponding to the decay of the first excited beryllium state were considered in the proposed approach.

Results from the full calculation up the 15 MeV is reported in Fig. 5, remarking that it is not used througout the complete energy range, obviously due to the local validity of the Breit-Wigner one level formula near the resonance.

4.4. *Collecting continuum and resonant contributions of* $^{11}B(p,\alpha_1)^{8}Be^{*}(3.03)$ *reaction*

A combination of the continuum theory and the Breit-Wigner resonance model was used to obtain a smooth cross section curve modeling the experimental data from theoretical considerations. The interval between isolated resonances was filled with the continuum reaction cross section for the $l = 0$ and $l = 1$ angular momentum protons, obtaining the results reported in Fig. 6. The Hale smooth fitting was made in 1979 as a private communication to the Los Alamos National Laboratory, University of California, and is contained in the Los Alamos Scientific Laboratory Reports, number 7066-PR, page 2, 1977/12 as a brief note. It consists of an evaluation from the measurements at California Institute of Technology (Davidson et al., 1979) for proton energies between 50 keV and 1.5 MeV, and by Segel et al. (1965) for proton energies below 3 MeV.

5. Conclusions

Theoretical nuclear models were studied, with the aim of approximating the reaction cross section for the proton-boron fusion. This nuclear reaction has been experimentally characterized over the years, and corresponding fittings and theoretical approximations for the alpha spectra are available in literature. In this work, a first principle approximation of the reaction cross section for the continuum and resonant parts of the excitation function $\sigma(E)$ is proposed. This information is valuable for determining the rate of ocurrence of the reaction, and might help to approximate a deconvolution of the physical dose absorbed in biological tissue due to the alpha particles emitted when making irradiation with protons, mainly for therapeutic purposes.

Acknowledgements

The author F.A. Geser would like to thank CONICET (Consejo Nacional de Investigaciones Científicas y Técnicas), Argentina, for the Ph.D. fellowship granted by resolution Nr D 4830.

References

Abramowitz, M., Stegun, I.A., 1964. Handbook of Mathematical Functions with Formulas, Graphs, and Mathematical Tables, 1st ed. United States Department of Commerce, National Bureau of Standards (NBS) (ISBN 0486612724,9780486612720).
Ajzenberg-Selove, F., 1990. Energy levels of light nuclei A = 11–12. Nucl. Phys. A 506 (1), 1–158. https://doi.org/10.1016/0375-9474(90)90271-m.
Becker, H.W., et al., 1987. Low-energy cross sections for 11B(p,3α). Z. für Phys. A At. Nucl. 327 (3), 341–355. https://doi.org/10.1007/BF01284459.
Bertulani, C.A., 2013. Nuclear reactions. In: Nuclei in the Cosmos, pp. 129–174. https://doi.org/10.1142/9789814417679_0005.
Blatt, J.M., Weisskopf, V.F., 1979. Theoretical Nuclear Physics. Springer-Verlag, New York, United States. https://doi.org/10.1007/978-1-4612-9959-2. (ISBN 978-1-4612-9961-5,978-1-4612-9959-2).
Cirrone, G.A.P., 2018. First experimental proof of proton boron capture therapy (PBCT) to enhance protontherapy effectiveness. Sci. Rep. 8. https://doi.org/10.1038/s41598-018-19258-5.
Cohen-Tannoudji, C., Diu, B., Laloë, F., 2006. Quantum Mechanics. Wiley, New York, United States (ISBN 9782705683931,9782705658342).
Davidson, J.M., et al., 1979. Low energy cross sections for 11B(p,3α). Nucl. Phys. A 315 (1–2), 19–26. https://doi.org/10.1016/0375-9474(79)90647-x.
Dmitriev, D., 2009. α-particle spectrum in the reaction $p + ^{11} B \rightarrow \alpha + ^{8} Be^{*} \rightarrow 3\alpha^{*}$. Phys. At. Nucl. 72 (7), 1165–1167. https://doi.org/10.1134/S1063778809070084.
Garcia, J., Galindo, A., 1991. Quantum Mechanics II. Theoretical and Mathematical Physics. Springer Berlin, Heidelberg (ISBN 9783642838569).
Kelley, J., et al., 2017. Energy levels of light nuclei A = 12. Nucl. Phys. A 968, 71–253. https://doi.org/10.1016/j.nuclphysa.2017.07.015.
Merzbacher, M., 1998. Quantum Mechanics. Wiley (ISBN 9780471887027).
Oliphant, M.L.E., Rutherford, L., 1933. Experiments on the transmutation of elements by protons. Proc. Math. Phys. Eng. Sci. 141, 259–281 (ISSN 1364-5021,1471-2946) http://dx.doi.org/10.1098%2Frspa.1933.0117.
Petringa, G., et al., 2017. Study of gamma-ray emission by proton beam interaction with injected boron atoms for future medical imaging applications. J. Instrum. 12, C03049 (URL https://doi.org/10.1088%2F1748-0221%2F12%2F03%2FC03049doi:10.1088%2F1748-0221%2F12%2F03%2FC03049 ISSN 1748-0221).
Segel, R.E., et al., 1965. States in C^{12} between 16.4 and 19.6 MeV. Phys. Rev. 139, B818–B830. https://doi.org/10.1103/PhysRev.139.B818.
Shin, H.B., et al., 2016. Prompt gamma ray imaging for verification of proton boron fusion therapy: a Monte Carlo study. Phys. Med. 32 (10), 1271–1275. https://doi.org/10.1016/j.ejmp.2016.05.053.
Stock, R., 2009. Encyclopedia of Applied High Energy and Particle Physics. Encyclopedia

of Applied Physics. Wiley, Weinheim, Germany (ISBN 9783527406913).
Vogel, J., et al., 2017. Proton therapy for pediatric head and neck malignancies. Pediatr. Blood Cancer 65 (2), e26858. https://doi.org/10.1002/pbc.26858.
Wang, M., et al., 2017. The AME2016 atomic mass evaluation (II).Tables, graphs and references. Chin. Phys. C. 41, 3(http://stacks.iop.org/1674-1137/41/i=3/a=030003).
Wong, S.S.M., 2007. Introductory Nuclear Physics, 2nd ed. WILEYVCH Verlag GmbH & Co. KGaA, Weinheim, Germany. https://doi.org/10.1002/9783527617906. (ISBN 9780471239734,9783527617906).
Yoon, D.K., et al., 2015. Application of proton boron fusion reaction to radiation therapy: a Monte Carlo simulation study. Appl. Phys. Lett. 105, 22. https://doi.org/10.1063/1.4903345.